Intelligent Automation & Soft Computing
DOI: 10.32604/iasc.2022.026052
Article

Tech Science Press

Extended Speckle Reduction Anisotropic Diffusion Filter to Despeckle Ultrasound Images

P. L. Joseph Raj, K. Kalimuthu*, Sabitha Gauni and C. T. Manimegalai

Department of ECE, College of Engineering and Technology, SRM Institute of Science and Technology, SRM Nagar, Kattankulathur, Tamil Nadu, India
*Corresponding Author: K. Kalimuthu. Email: kalimutk@srmist.edu.in
Received: 14 December 2021; Accepted: 25 January 2022

Abstract: Speckle Reduction Anisotropic Diffusion filter which is used to despeckle ultrasound images, perform well at homogeneous region than in heterogeneous region resulting in loss of information available at the edges. Extended SRAD filter does the same, preserving better the edges in addition, compared to the existing SRAD filter. The proposed Extended SRAD filter includes the intensity of four more neighboring pixels in addition with other four that is meant for SRAD filter operation. So, a total of eight pixels are involved in determining the intensity of a single pixel. This improves despeckling performance by maintaining the information accessible at an image's edges. The proposed filter produces better Peak Signal to Noise Ratio, Root Mean Square Error and Structural Similarity Index values for standard test images with different noise levels with variance 0.3, 0.35 and 0.4. It also performs well in denoising breast ultrasound images at different noise levels.

Keywords: SRAD filter; despeckling; PSNR; RMSE; SSI

1 Introduction

X ray, Ultrasound, Computer Tomography (CT) and Magnetic Resonance Imaging (MRI) are the most commonly used medical imaging modalities. Among these four modalities, ultrasound is widely used [1]. These modalities provide images with noise that is introduced during their acquisition [2], especially in the fields of follicle detection [3], detection of fetal gestational age [4], along with any kind of automatic Active Contour Model (ACM) for segmentation [5]. Ultrasound images contain speckle noise that is equivalent to the noise that occurs in the Synthetic Aperture Radar (SAR) images. Speckle noise causes serious problem in the image recognition as it has a cumulative effect and might lead to incorrect conclusions [6]. Image analysis is difficult when speckle noise is present and the process of its removal from the SAR images result in loss of information available at the edges of the image [7]. This may be avoided by employing the Discrete Wavelet Transform (DWT) [8] technique after the image is filtered by a preprocessing filter [9]. Recently, research based on the use of filters in conjunction with various clustering or optimization techniques have been accessible. M3 filter along with clustering is also used for identifying the region of interest in ultrasound images [10]. Adaptive denoising technique combined

with cuckoo search optimization is implemented for depeckling the ultrasound images [11]. However, these methods are computationally complex and time consuming.

Lee filter, Frost filter, Guided filter and Speckle Reduction Anisotropic Diffusion (SRAD) filter are most commonly used filters in depeckling the ultrasound images. Peak Signal to Noise Ratio (PSNR) and Structural Similarity Index (SSI) values of the images are obtained for various filters and compared to analyze their performance. Among these filters, SRAD filter perform well compared to others in the case of image enhancement and denoising [12]. They smoothen the images and enhance the edges by inhibiting diffusion across the edges allowing isotropic diffusion within the homogenous region. The SRAD filtered resulting image consists of two parts such as useful signal and noise. The former is caused by the effect of the medical ultrasonic imaging principle while the latter is generated by the sensor available in the imaging probe, consisting both multiplicative and additive noise. The speckle noise model of the SRAD resulting image is expressed as Eq. (1), in which $O(x, y)$, $W(x, y)$ and $A(x, y)$ are the original, multiplicative and additive noises respectively [13].

$$F(x,\ y) = O(x,\ y) \times W(x,\ y) + A(x,\ y) \tag{1}$$

Existing filters other than SRAD filter do not enhance edges; they only inhibit smoothening near the edges [14]. In spite of its advantages, SRAD filter loses information at the edges while processing an image. SRAD filter in association with guided filter works in speckle noise reduction and preservation of edges as well effectively [15]. After preprocessing and using DWT, the sample picture is transformed into one approximate sub band image and six detailed sub band images. The available diagonal sub band images are made to pass through the Improved Guided Filter (IGF) in order to the additive noise present while still preserving the information available in the edges [16].

Soft and hard threshold are the wavelet functions that are most commonly used in image processing. These two are responsible in the speckle noise reduction in SAR images. Normally, both threshold values are zero, and no fluctuation in the noise value is allowed [17]. Soft threshold function suppresses the coefficients that are larger than its reference value whereas hard threshold function does not act in this condition. But if the coefficients are lesser than the threshold value, hard threshold function removes them [18].

2 Speckle Reduction Anisotropic Diffusion Filter

Speckle noise available in an image can be removed by applying a Partial Differential Equation (PDE) approach, inculcated in SRAD filter. This filter is most commonly used in ultrasonic and radar imaging applications. Even with the basic anisotropic diffusion filter, edge sensitive diffusion for images with additive noise is conceivable, whereas SRAD filters are very much used in the case of image with multiplicative noise (Speckled image). Perona et al. have developed anisotropic diffusion which is considered to be an average filter's edge sensitive extension [19] whereas SRAD is found to be conventional adaptive speckle filter's edge sensitive extension. SRAD filter applies diffusion technique based on the Minimum Mean Square Error (MMSE) approach which makes it work similar to Lee filter and Frost filter as they too utilize the same approach. The difference between SRAD and the other two filters is, the latter use coefficient of variation in their operation and the former utilize the function of local gradient magnitude and Laplacian operator known as the image's instantaneous coefficient of variation. Anisotropic diffusion in SRAD filter is different and advantageous with respect to conventional anisotropic diffusion. Even though it performs normally while working in the centre of an edge, it impacts negative diffusion along the edge direction on both sides of the edge [20]. This results in sharper edge contour that makes dark side of an edge darker and brighter side of an edge even brighter.

3 Extended SRAD Filter

The SRAD filter [9] is replaced by extended SRAD filter in order to obtain better results with respect to performance metrics namely PSNR, Root Mean Square Error (RMSE) and SSI. The block diagram of the proposed method is depicted in Fig. 1. The only difference between block diagram of the existing and the proposed method is the filter used. SRAD filter is used in the existing method which is replaced by extended SRAD filter in the proposed method. The proposed block diagram consists of extended SRAD filter, log transform block, wavelet transform block, sub band imaging block, soft thresholding block, inverse wavelet transform and exponential transform block.

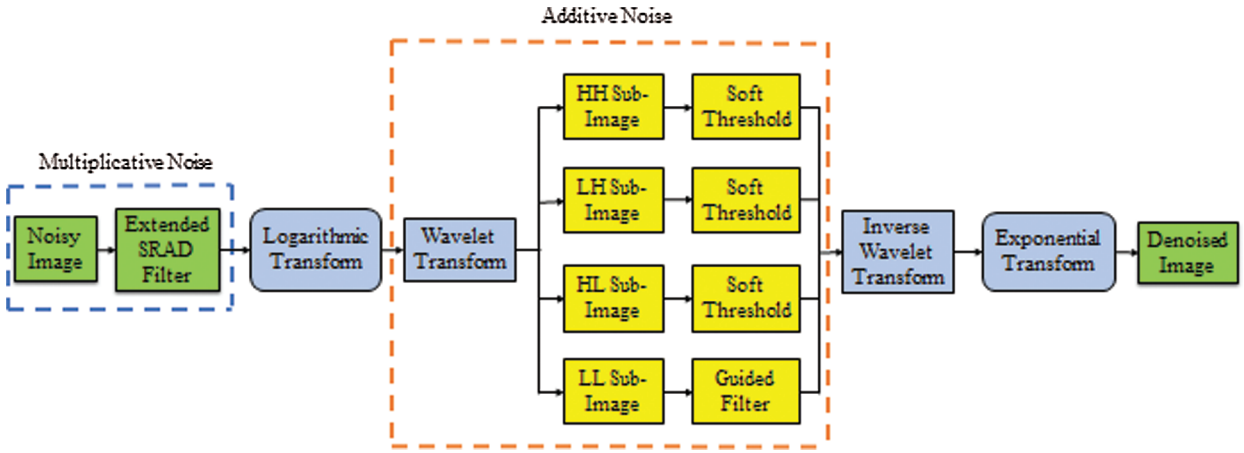

Figure 1: Block diagram of the proposed method

Noisy image applied as input to the extended SRAD filter is obtained by adding multipicative noise to it. It is then filtered by extended SRAD operation. Logarithmic and wavelet transformations are applied over the filter output which is then subdivided into four sub band images namely High High (HH), Low High (LH), High Low (HL) and Low Low (LL). Soft thresholding is done over the first three sub band images whereas LL sub band image is filtered by guided filter. Inverse Wavelet Transform (IWT) is applied over the combined output of soft thresholding and guided filter blocks. Exponential transform is applied as an inverse operation of logarithmic transform to obtain the denoised image at the output end.

It is further developed by working on the following set of equations. The Partial Differential Equation (PDE) model of anisotropic diffusion filter is given by [14] and it is shown in Eq. (2).

$$\begin{cases} \dfrac{\partial I}{\partial t} = div[c(q).\nabla I] \\ I(t=0) = I_0. \end{cases} \tag{2}$$

The below equation is obtained by applying Jacobi iterative method over the Eq. (2),

$$I_{i,j}^{n+1} = I_{i,j}^{n} + \left(\frac{\Delta t}{8}\right) d_{i,j}^{n}. \tag{3}$$

Actually, the solution of the existing SRAD filter has only four components in it that denotes the nature of the pixels to the north, south, east, and west of the corresponding pixel to be processed as per its design. To boost its performance even further four more neighboring pixels located at the North east, North west, South east and South west are also considered for computation, in the proposed extended algorithm. Hence, the divergence gets added with 4 more components given by,

$$d_{i,j}^n = c_{i,j}^n(I_{i-1,j}^n - I_{i,j}^n) + c_{i+1,j}^n(I_{i+1,j}^n - I_{i,j}^n) + c_{i,j}^n(I_{i,j-1}^n - I_{i,j}^n) + c_{i,j+1}^n(I_{i,j+1}^n - I_{i,j}^n) + c_{i,j}^n(I_{i-1,j-1}^n - I_{i,j}^n) + c_{i,j+1}^n(I_{i-1,j+1}^n - I_{i,j}^n) + c_{i+1,j}^n(I_{i+1,j-1}^n - I_{i,j}^n) + c_{i+1,j+1}^n(I_{i+1,j+1}^n - I_{i,j}^n). \quad (4)$$

Here diffusion coefficient c (q) is defined as [8],

$$c(q) = \exp\left\{-\frac{[q^2 - q_0^2]}{[q_0^2(1+q_0^2)]}\right\} \quad (5)$$

$$q = \sqrt{\frac{\left(\frac{1}{4}\right)\left(\frac{|\nabla I|}{I}\right)^2 - \left(\frac{1}{8^2}\right)\left(\frac{|\nabla^2 I|}{I}\right)^2}{\left[1 + \left(\frac{1}{8}\right)\left(\frac{|\nabla^2 I|}{I}\right)\right]^2}}. \quad (6)$$

Instantaneous coefficient of variation q is obtained by applying Eqs. (7) and (8) in Eq. (5).

$$\frac{|\nabla^2 I_{i,j}^n|}{I_{i,j}^n} = \frac{1}{I_{i,j}^n}[I_{i-1,j}^n + I_{i+1,j}^n + I_{i,j-1}^n + I_{i,j+1}^n + I_{i-1,j-1}^n + I_{i-1,j+1}^n + I_{i+1,j-1}^n + I_{i+1,j+1}^n - 8I_{i,j}^n] \quad (7)$$

$$\left(\frac{|\nabla I_{i,j}^n|}{I_{i,j}^n}\right)^2 = \frac{1}{(I_{i,j}^n)^2}\left[\begin{array}{l}(I_{i-1,j}^n - I_{i,j}^n)^2 + (I_{i+1,j}^n - I_{i,j}^n)^2 + (I_{i,j-1}^n - I_{i,j}^n)^2 + (I_{i,j+1}^n - I_{i,j}^n)^2 + (I_{i-1,j-1}^n - I_{i,j}^n)^2 \\ +(I_{i-1,j+1}^n - I_{i,j}^n)^2 + (I_{i+1,j-1}^n - I_{i,j}^n)^2 + (I_{i+1,j+1}^n - I_{i,j}^n)^2\end{array}\right] \quad (8)$$

Eq. (3) is the extended version of the existing SRAD filter. The solution of the same is the result of the proposed extended algorithm with 8 coefficients. Breast ultrasound images filtered by the proposed filter have been obtained from Breast Ultrasound Lesions Dataset (Dataset B) [21].

4 Results and Discussion

SRAD filter is most commonly used in processing Synthetic Aperture Radar (SAR) images. In this research work, all the available despeckling filters namely, Lee filter, Frost filter, Guided filter, SRAD filter, Speckle Reduction Anisotropic Diffusion Guided Filter (SRAD GF), Speckle Reduction Anisotropic Diffusion Improved Guided Filter (SRAD IGF) and the proposed extended SRAD filter are operated to denoise three standard test images namely Cameraman©, House© and Lena© with different noise levels of variance 0.3, 0.35 and 0.4 (refer, Figs. 2–5) and their respective performance metrics such as PSNR, RMSE and SSI were determined.

(a) (b) (c)

Figure 2: Original test images with 512 × 512 pixels: (a) Cameraman (b) House (c) Lena

(a) (b) (c)

Figure 3: Cameraman Image: (a) Original (b) With noise variance 0.3 (c) Denoised output using extended SRAD filter

(a) (b) (c)

Figure 4: Cameraman Image: (a) Original (b) With noise variance 0.35 (c) Denoised output using extended SRAD filter

(a) (b) (c)

Figure 5: Cameraman Image: (a) Original (b) With noise variance 0.4 (c) Denoised output using extended SRAD filter

When the noise variance is 0.3, the proposed extended SRAD filter performs well in the case of standard images (Cameraman, House, Lena) exhibiting better values than the existing filters with respect to performance metrics namely PSNR, RMSE and SSI. It is clear that the suggested expanded SRAD filter produces better results for the House picture than for the Cameraman and Lena photos (Refer, Tabs. 1–3)

Table 1: Peak signal to noise ratio (PSNR) values for noise variance 0.3

Images	Noisy	GF	LEE	FROST	SRAD	SRAD-GF	SRAD-IGF	Extended SRAD filter
Cameraman	20.864	26.524	26.266	26.219	26.226	28.276	28.944	30.172
House	20.201	30.362	29.876	29.685	25.701	29.946	29.745	32.619
Lena	20.943	27.315	27.434	27.271	26.141	28.509	28.569	29.903

Table 2: Root mean square error (RMSE) values for noise variance 0.3

Images	Noisy	GF	LEE	FROST	SRAD	SRAD-GF	SRAD-IGF	Extended SRAD filter
Cameraman	0.091	0.047	0.049	0.034	0.049	0.039	0.036	0.031
House	0.098	0.030	0.032	0.022	0.052	0.032	0.033	0.023
Lena	0.090	0.043	0.042	0.030	0.049	0.038	0.037	0.032

Table 3: Structural similarity index (SSI) values for noise variance 0.3

Images	Noisy	GF	LEE	FROST	SRAD	SRAD-GF	SRAD-IGF	Extended SRAD filter
Cameraman	0.420	0.812	0.830	0.708	0.579	0.733	0.738	0.857
House	0.281	0.874	0.887	0.795	0.505	0.747	0.735	0.875
Lena	0.362	0.772	0.782	0.495	0.559	0.731	0.728	0.809

When the noise variance is 0.35, the proposed extended SRAD filter performs well in the case of standard images (Cameraman, House, Lena) exhibiting better values than the existing filters with respect to performance metrics namely PSNR, RMSE and SSI. It is visible that proposed extended SRAD filter yields better results for House image compared to Cameraman and Lena images. (Refer, Tab. 4). SRAD GF performs slightly better than SRAD IGF in terms of PSNR for some of the standard images.

Table 4: Performance metrics for noise variance 0.35

Images	PSNR				RMSE				SSI			
	Noisy	SRAD-GF	SRAD-IGF	extended SRAD filter	Noisy	SRAD-GF	SRAD-IGF	extended SRAD filter	Noisy	SRAD-GF	SRAD-IGF	extended SRAD filter
Cameraman	20.230	28.101	28.691	30.058	0.097	0.039	0.037	0.031	0.404	0.716	0.720	0.850
House	19.602	29.560	29.323	32.241	0.105	0.033	0.034	0.024	0.259	0.730	0.717	0.866
Lena	20.323	28.256	28.286	29.704	0.096	0.039	0.039	0.033	0.340	0.715	0.711	0.803

When the noise variance is 0.4, the proposed extended SRAD filter performs well in the case of standard images (Cameraman, House, Lena) exhibiting better values than the existing filters with respect to performance metrics namely PSNR, RMSE and SSI. It is visible that proposed extended SRAD filter yields better results for House image compared to Cameraman and Lena images. (Refer, Tab. 5). SRAD GF performs slightly better than SRAD IGF in terms of SSI for some of the standard images.

Table 5: Performance metrics for noise variance 0.4

Images	PSNR				RMSE				SSI			
	Noisy	SRAD-GF	SRAD-IGF	extended SRAD filter	Noisy	SRAD-GF	SRAD-IGF	extended SRAD filter	Noisy	SRAD-GF	SRAD-IGF	extended SRAD filter
Cameraman	19.628	27.815	28.343	29.804	0.104	0.041	0.038	0.032	0.389	0.696	0.700	0.839
House	19.121	29.253	28.977	31.960	0.111	0.034	0.036	0.025	0.242	0.717	0.701	0.859
Lena	19.748	28.031	28.035	29.545	0.103	0.040	0.040	0.033	0.321	0.698	0.693	0.795

The main purpose of the research work is to enhance the quality of the medical ultrasound images. In this regard, two breast ultrasound images were filtered using the existing filters and also with the proposed extended SRAD filter (see Figs. 6 and 7). Suspicious masses present in the female breasts are to be evaluated by obtaining its ultrasound image [22]. The images were added with noise level of variance 0.3, before they were filtered and their performance metrics were measured.

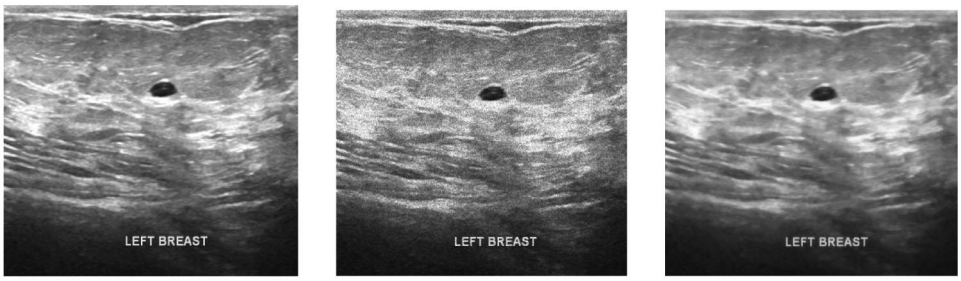

(a) (b) (c)

Figure 6: Breast Ultrasound image (Benign): (a) Original (b) With noise variance 0.3 (c) Denoised output using extended SRAD filter

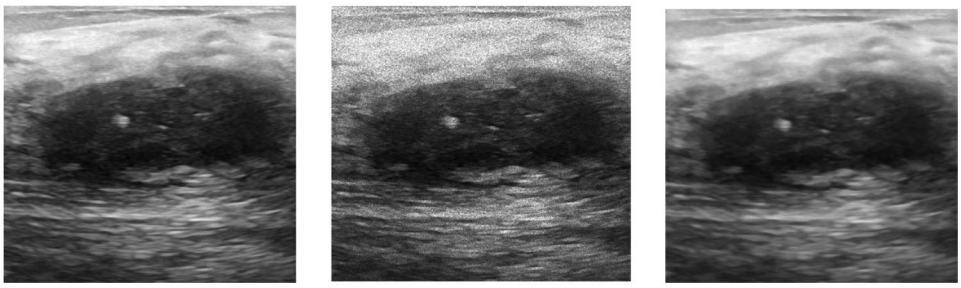

(a) (b) (c)

Figure 7: Breast Ultrasound image (Malignant): (a) Original (b) With noise variance 0.3 (c) Denoised output using extended SRAD filter

When the noise variance is 0.3, the proposed extended SRAD filter performs well over both the noisy medical images (Benign, Malignant) exhibiting better values than the existing filters with respect to performance metric PSNR. It is visible that proposed extended SRAD filter yields better result for malignant image compared to benign. (Refer, Tab. 6)

Table 6: Peak signal to noise ratio (PSNR) values for noise variance 0.3

Images	Noisy	GF	LEE	FROST	SRAD	SRAD-GF	SRAD-IGF	Extended SRAD filter
Benign	20.497	27.111	26.396	26.220	25.792	27.214	26.761	28.573
Malignant	21.267	28.083	28.165	28.064	26.693	28.572	28.188	29.943

When the noise variance is 0.3, the proposed extended SRAD filter performs well over both the noisy medical images (Benign, Malignant) exhibiting better values than the existing filters with respect to performance metric RMSE. It is visible that proposed extended SRAD filter yields better result for malignant image compared to benign. (Refer, Tab. 7)

Table 7: Root mean square error (RMSE) values for noise variance 0.3

Images	Noisy	GF	LEE	FROST	SRAD	SRAD-GF	SRAD-IGF	Extended SRAD filter
Benign	0.094	0.044	0.048	0.034	0.051	0.044	0.046	0.037
Malignant	0.086	0.039	0.039	0.027	0.046	0.037	0.039	0.032

When the noise variance is 0.3, the proposed extended SRAD filter performs well over both the noisy medical images (Benign, Malignant) exhibiting better values than the existing filters with respect to performance metric SSI. It is visible that proposed extended SRAD filter yields better result for benign image compared to malignant. (Refer, Tab. 8) After the noise is added to the image to be processed, it is made to undergo preprocessing through each of the various filters namely Guided filter, LEE filter, FROST filter, SRAD filter, SRAD GF, SRAD IGF and extended SRAD filter, one at a time. Except the proposed filter named as extended SRAD filter the remaining are existing filters.The proposed extended SRAD filter performs well ahead than the existing filters in the case of both standard images and medical ultrasound images as well. It is witnessed from the filtered output images and their metric values.

Table 8: Structural similarity index (SSI) values for noise variance 0.3

Images	Noisy	GF	LEE	FROST	SRAD	SRAD-GF	SRAD-IGF	Extended SRAD filter
Benign	0.379	0.727	0.740	0.477	0.636	0.719	0.705	0.784
Malignant	0.422	0.722	0.739	0.540	0.655	0.709	0.703	0.778

5 Conclusion

SRAD filters are good in despeckling SAR images. It is also used to despeckle ultrasound images which are affected by speckle noise to a larger extent. The performance of SRAD filter at the edges of an image (Heterogeneous) is less compared to the smoother section of the image (Homogeneous). This drawback is addressed in this research by designing and implementing an extended SRAD filter whose performance is found to be better by yielding 30.172 PSNR, 0.031 RMSE, 0.857 SSI for standard camera man image and in the case of malignant breast ultra sound image, the proposed extended SRAD filter yields 29.943 PSNR, 0.032 RMSE, 0.778 SSI than the conventional SRAD filter, especially in preserving the

edges. The proposed extended SRAD filter overcomes this drawback by preserving the edges with minimum loss of information at the edges with better performance metrics.

The proposed extended SRAD filter involves 8 coefficients in computing the performance metrics such as PSNR, RMSE and SSI resulting in better output, trading off the time taken for its computation compared to the computation time with respect to 4 coefficients. The scope of future work is to improve the computation time of the extended SRAD filter.

Funding Statement: The authors received no specific funding for this study.

Conflicts of Interest: The authors declare that they have no conflicts of interest to report regarding the present study.

References

[1] M. A. Yousuf and M. N. Nobi, "A new method to remove noise in magnetic resonance and ultrasound images," *Journal of Scientific Research*, vol. 3, no. 1, pp. 81–81, 2011.

[2] P. B. Alisha and K. G. Sheela, "Image denoising techniques-an overview," *IOSR Journal of Electronics and Communication Engineering*, vol. 11, no. 1, pp. 78–84, 2016.

[3] P. S. Hiremath and J. R. Tegnoor, "Fuzzy inference system for follicle detection in ultrasound images of ovaries," *Soft Computing*, vol. 18, pp. 1353–1362, 2014.

[4] S. Meenakshi, M. Suganthi and P. Suresh Kumar, "An approach for automatic detection of fetal gestational age at the third trimester using kidney length and biparietal diameter," *Soft Computing*, vol. 23, pp. 2839–2848, pp. 78–2884, 2016.

[5] L. Fang, X. Pan and Y. Yao, "A hybrid active contour model for ultrasound image segmentation," *Soft Computing*, vol. 24, pp. 18611–18625, 2020.

[6] F. Gao, X. Xue, J. Sun, J. Wang and Y. Zhang, "A SAR image despeckling method based on two-dimensional S transform shrinkage," *IEEE Transactions on Geoscience and Remote Sensing*, vol. 54, no. 5, pp. 3025–3034, 2016.

[7] G. Othman and D. Q. Zeebaree, "The applications of discrete wavelet transform in image processing: A review," *Journal of Soft Computing and Data Mining*, vol. 1, no. 2, pp. 31–43, 2020.

[8] D. Al-Karawi, D. Ibrahim, H. Al-Assam, H. B. Du and S. Jassim, "A Model-based adaptive method for speckle noise reduction in ultrasound images of ovarian tumours: A new approach," *Multimodal Image Exploitation and Learning*, vol. 11734, pp. 117340J, 2021.

[9] H. Choi and J. Jeong, "Despeckling images using a preprocessing filter and discrete wavelet transform-based noise reduction techniques," *IEEE Sensors Journal*, vol. 18, no. 8, pp. 3131–3139, 2018.

[10] K. Thangavel and R. Manavalan, "Soft computing models-based feature selection for TRUS prostate cancer image classification," *Soft Computing*, vol. 18, pp. 1165–1176, 2014.

[11] M. Malik, F. Ahsan and S. Mohsin, "Adaptive image denoising using cuckoo algorithm," *Soft Computing*, vol. 20, pp. 925–938, 2016.

[12] S. Kushwaha and R. K. Singh, "Performance comparison of different despeckled filters for ultrasound images," *Biomedical and Pharmacology Journal*, vol. 10, no. 2, pp. 837–845, 2017.

[13] H. Choi and J. Jeong, "Despeckling algorithm for removing speckle noise from ultrasound images," *Symmetry*, vol. 12, no. 6, pp. 938, 2020.

[14] Y. Yu and S. T. Acton, "Speckle reducing anisotropic diffusion," *IEEE Transactions on Image Processing*, vol. 11, no. 11, pp. 1260–1270, 2002.

[15] H. Choi and J. Jeong, "Speckle noise reduction in ultrasound images using SRAD and guided filter," in *2018 Int. Workshop on Advanced Image Technology (IWAIT)*, Chiang Mai, Thailand, pp. 1–4, 2018.

[16] H. Choi and J. Jeong, "Speckle noise reduction technique for SAR images using statistical characteristics of speckle noise and discrete wavelet transform," *Remote Sensing*, vol. 11, no. 10, pp. 1184, 2019.

[17] M. Biswas and H. Om, "A new soft-thresholding image denoising method," *Procedia Technology*, vol. 6, pp. 10–15, 2012.

[18] S. G. Chang, B. Yu and M. Vetterli, "Adaptive wavelet thresholding for image denoising and compression," *IEEE Transactions on Image Processing*, vol. 9, no. 9, pp. 1532–1546, 2000.

[19] P. Perona and J. Malik, "Scale-space and edge detection using anisotropic diffusion," *IEEE Transactions on Pattern Analysis and Machine Intelligence*, vol. 12, no. 7, pp. 629–639, 1990.

[20] S. Goyal, A. Rani, N. Yadav and V. Singh, "SGS-SRAD filter for denoising and edge preservation of ultrasound images," in *6th Int. Conf. on Signal Processing and Integrated Networks (SPIN)*, Noida, India, pp. 676–682, 2019.

[21] M. H. Yap, G. Pons, J. Marti, S. Ganau, M. Sentis *et al.,* "Automated breast ultrasound lesions detection using convolutional neural networks," *IEEE Journal of Biomedical and Health Informatics*, vol. 22, no. 4, pp. 1218–1226, 2017.

[22] N. Ozmen, R. Dapp, M. Zapf, H. Gemmeke, N. V. Ruiter *et al.,* "Comparing different ultrasound imaging methods for breast cancer detection," *IEEE Transactions on Ultrasonics, Ferroelectrics, and Frequency Control*, vol. 62, no. 4, pp. 637–646, 2015.